

# Morphological, and Optical Properties of BaTiO<sub>3</sub> Nano Particles

**Dr. P. Laveena Manjulatha**

Assistant Professor of Physics, HoD Department of Physics, MALDGdcgadwal, Palamuru university, Telangana, India

## Abstract

Barium titanate (BaTiO<sub>3</sub>) nano particles have garnered significant attention due to their unique structural, morphological and optical properties, which hold promise for various technological applications. This study presents a comprehensive investigation in to the synthesis potential of BaTiO<sub>3</sub> nano particle. The synthesis of BaTiO<sub>3</sub> nano particles was achived through various methods, including sol-gel, hydrothermal, and solvothermal routes, with meticulous control over parameters such as temperature, pH, and precursor concentration to tailor the nano particle size and morphology. The structural characterization using techniques such as x-ray diffraction (XRD) revealed the formation of pure –phase BaTiO<sub>3</sub>nanoparticles with crystallite sizes in the nanometer range, exhibiting a perovskite strucure. Morphological analysis using scanning electron microscopy (SEM) and transmission electron microscopy (TEM) elucidated the morphology, size distribution, and surface chacteristics of the nano particles. The results showcased well – defined, uniform nano particles with controllable sizes and shapes, ranging from spherical to cubic, depending onthe synthesis conditions. futher more, the optical properties ofBaTiO<sub>3</sub> nanoparticles were investigated using UV-visible spectroscopy and photoluminescence spectroscopy. The UV- visible spectra exhibited characteristic absorption peaks corresponding to the electronic transitions within the band structure of BaTio<sub>3</sub>,while photoluminescence spectra revealed emission peaks indicative of defect states with in the nanoparticle. These optical properties were found to be tunable by varying the nano particle size, morphology, and surface characteristics, offering opportunities for optoelectronic and photonic device applications. The key findings of this study underscore the importance of understanding the interplay between synthesis parameters and resulting structural, morphological, and optical properties of BaTiO<sub>3</sub> nanoparticles.

**Keywords:** Barium titanate nanoparticles, synthesis, structural characterization, morphological and Analysis, optical properties, nanotechnology.

## Introduction:

Nanoparticle synthessis techniques have more prominence than the bulk synthesis technique owing to their potential applications in biomedical sciences, drug delivery systems, sensors, nanofibers, carbon nanotubes, quantun dots, photocatalysis, dielectric, ferroelectric and piezoelectric properties [1].

In general, Barium Titanate (BT) is a promising dielectric material and shows tremondous applications as

multilayer ceramic capacitors (MLCC) due to decrease of particle size [2]. The reduction in particle size can be attributed to the usage of low operating temperatures while conducting the synthesis part of work. The significance behind the low temperature synthesis techniques were achieving the high purity, homogeneous and ultrafine nanoparticles [2]. Several researchers prepared BT nanoparticles via distinct methods such as hydrothermal [2], sol-gel [3], micro-emulsion [4], polymeric precursor [5] and microwave heating [6]. All the above stated techniques focussed on the structural, morphological, Raman & IR-spectra, UV-visible spectra, dielectric and ferroelectric properties. More recently Selvarajan et al. [7], prepared the piezoelectric BT nanoparticles and proposed that it can be used as an active biosensor for the biomolecular detection via the conventional-solid state reaction method. In addition to these, Singh et al. [8] experimentally showed that the perovskite BT thinfilm is an effective material for LPG sensor. According to the literature survey, BT nanoparticles are mainly focussed to reveal the biomedical and sensor applications. Therefore, in the current investigation, the authors have focussed their attention to elucidate the structural, morphological and optical properties of BT microspheres.

### Sample Preparation:

Barium Titanate nanoparticles have been synthesized by adopting the Hydrothermal method in the present investigation, since it is more feasible and more advantages over conventional method. The details of the method are given in chapter II. In order to synthesize barium titanate nanoparticles the starting materials have been chosen as Ba (NO<sub>3</sub>)<sub>2</sub> and TiO<sub>2</sub> (each of 99.9 % purity, Sigma-Aldrich). These precursors have been mixed together after taking their stoichiometric ratio. The whole mixed precursors have been transferred to glass beaker. Further more distilled water has been added to the precursors in the ratio of 1:4 (mixed precursors (gm): distilled water (ml)) and the resultant solution has been kept on a magnetic stirrer. This stirring rate of 500 rpm has been maintained in order to stir the solution. Later NaOH solution is slowly added and the p<sup>H</sup> value reached to 11.3. Further more this solution is transferred to 300 ml Teflon bowl inserted in an autoclave. The sealed autoclave is kept in a hot-air oven at an operating temperature of 130°C/6 hrs. After completion of the reaction the autoclave was slowly cooled to room temperature. The final BaTiO<sub>3</sub> nano-particles were removed from the Teflon lined autoclave and washed with acetone and distilled water for 10 to 12 times until the p<sup>H</sup> is reduced to 7. The final BT nanoparticles were removed and characterized for various characterized techniques such as X-ray diffraction method, field emission scanning and transition electron microscopy. In addition, the FTIR, UV visible techniques are used to find the presence of metal oxide bands and the optical energy band gap.

### Results and Discussions:

Various characterization techniques have been employed to study Structural, Morphological and Optical properties of newly synthesized nano particles in the present investigation are given below.

### XRD Analysis (Structural Property):

The diffraction pattern of BT nanoparticles is depicted in Fig.1. It can be seen that BT nanoparticles exhibit cubic perovskite structure pertaining to the reflection planes as indicated in Fig.1. These reflection planes are in good agreement with JCPDS data of file number: 89-2475. Among these planes the (110) plane at

31.55° revealed the maximum intensity. No secondary peaks are observed in BT structure. The average crystallite size ‘D<sub>p</sub>’ is evaluated with the help of average full-width at half-maxima (FWHM) of reflection planes using the Debye-Scherrer equation [9]

$$D_p = \frac{k\lambda}{Q \cos\theta} \quad (3.1.)$$

where β is full width half maxima, λ is wave length of CuK<sub>α</sub> radiation (0.1542 nm) and θ is diffraction angle and ‘K’ is a numerical constant which is equal to 0.9 for a spherical atom. The results are repeated in Table.1. It is clear from the table that the crystal size is varying from 4 to 45 nm. The average crystallite size is calculated to be 21 nm. Fig. 2 depicts the variation of crystallite size and micro strain as a function of diffraction angle. It is very clear from the figure that there exists a reciprocal relationship between microstrain and crystallite size. Similar kinds of observations were previously reported in the literature [13]. In addition, the lattice constant (a) is calculated after finding the inter-planer spacing (d) and miller indices (hkl) by using the following formula [10]:

$$a = d(h^2 + k^2 + l^2)^{1/2} \quad (3.2.)$$

The lattice parameter is found to be 4.007 Å. This value is greater than the reported lattice constant of 3.972 Å for bulk BT material [11]. The X-ray density (D<sub>x</sub>) is evaluated using the formula  $ZM/Na^3$ , where ‘Z’ is the number of molecules per unit cell (Z=8), ‘M’ is the molecular weight of the composition, ‘N’ is Avogadro’s number (6.023 x 10<sup>23</sup>) and ‘a’ is the lattice parameter [10]. The numerical value of D<sub>x</sub> is observed to be 6.022 g/cm<sup>3</sup> which is larger than the X-ray density of bulk BT of 5.427 g/cm<sup>3</sup> [11]. This may be attributed to the high homogeneity of prepared BT nanoparticles. Moreover, the structural parameters such as interplanar-spacing (d), full width half maxima (FWHM), micro-strain (ε), miller indices (hkl) and dislocation density (ρ) are listed in Table.1 as a function of diffraction angle. The inter planar-spacing is decreasing with increase of 2θ degree angle. In addition, the dislocation density is a parameter that evaluates the defects per unit area of the sample. The smaller value of ρ indicates the low porous structure of BT nanoparticles and it is vice-versa. In the current study the average ρ is ~ 7.96 x 10<sup>15</sup> m<sup>-2</sup>. The micro strain at an average for all diffraction angles is noticed to be 0.0044. The specific surface area (S) is a significant physical parameter for nanoparticles and is computed using the relation: 6000/D<sub>p</sub>D<sub>x</sub>, where the symbols have their usual meaning [12]. In this study the S is achieved to be ~50 m<sup>2</sup>/g. This kind of high value of S can be attributed to the smallest value of crystallite size when compared with bulk materials. This larger S value in turn affects the electrical, optical and morphological properties of nanoparticles.

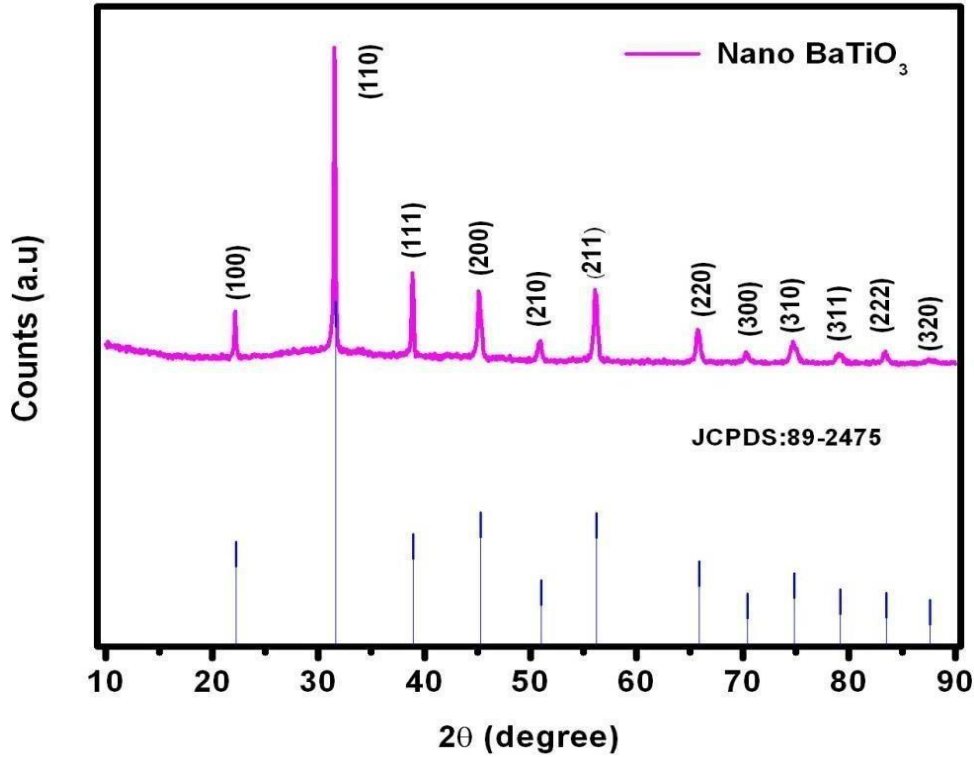


Fig.1 The diffraction pattern of BTnanoparticles

2θ(°)	FWHMβ(°)	d(Å)	E	Dp(nm)	Hkl	ρ(m <sup>-2</sup> )
22.173	0.221	4.006	0.0049	39	100	6.57E+14
31.548	0.175	2.834	0.0027	45	110	4.94E+14
38.861	0.21	2.316	0.0026	38	111	6.93E+14
45.174	0.441	2.006	0.0046	21	200	2.27E+15
50.861	0.546	1.794	0.0050	17	210	3.46E+15
56.112	0.37	1.638	0.0030	24	211	1.74E+15
65.737	0.464	1.419	0.0031	20	220	2.5E+15
70.3	0.869	1.338	0.0054	12	300	6.94E+15
74.737	0.777	1.269	0.0044	14	310	5.1E+15
79.05	0.951	1.211	0.0050	12	311	6.94E+15
83.425	0.472	1.158	0.0023	21	222	2.27E+15
87.488	3.119	1.114	0.0142	4	320	6.25E+16

Table.1 The data on structural and physical parameters of BTnanoparticles

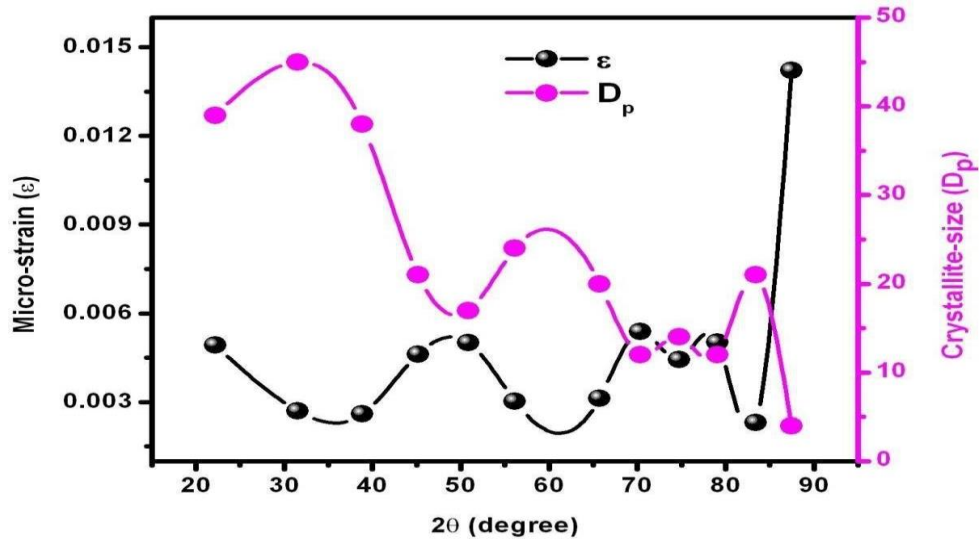


Fig.2 The variation of microstrain and crystallite size of BT nanoparticles

Williamson-Hall (W-H) plot (as shown in Fig.3.) is drawn for  $\beta \cos\theta$  versus  $4\sin\theta$  in order to evaluate micro-strain ( $\epsilon$ ) and crystallite size ( $D$ ) using the following relation [13].

$$\beta \cos\theta = \frac{0.9\lambda}{D} + 4\epsilon \sin\theta \quad (3.3)$$

$D$  where the slope of straight line offers micro-strain while, crystallite size is associated to intercept parameter. This provides the correlation between strain and size of the crystallite. The results from W-H plot express that the strain (0.0041) is almost consistent with the Scherrer strain from diffraction pattern. The average crystallite size is of order of 19.5 nm which is almost in agreement with the Scherrer size.

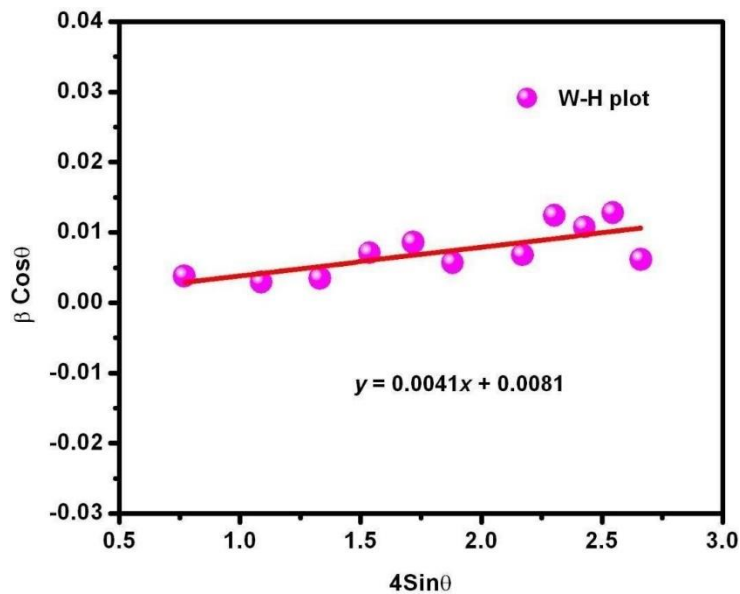
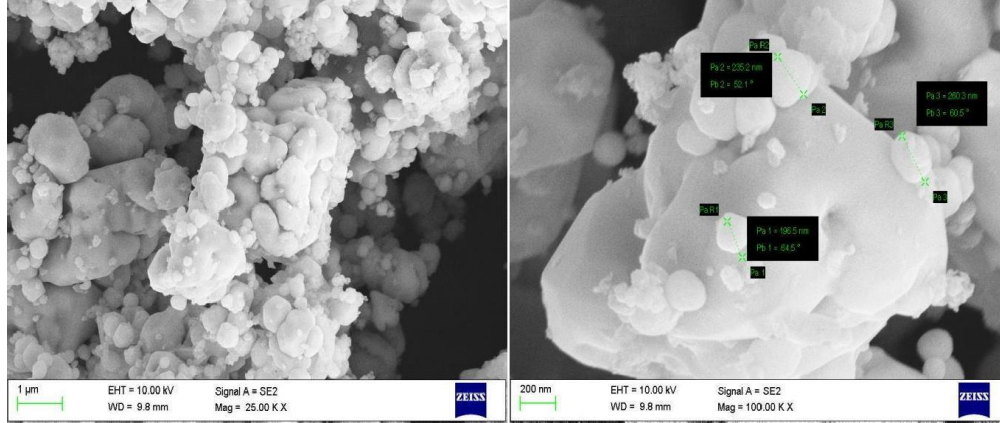


Fig.3. The W-H plot of BT nanoparticles

**2.a.FESEM Analysis(SurfaceMorphologyProperty):**

The surface morphology of BT nano-particles is analyzed by FESEM and TEM.The FE-SEM photographs of BT nano-particles are showed in Fig. 4.



**Fig.4The FESEM photos of BTnanoparticles**

From Fig.3.4,it is noticed that BT shows well defined spherical grains. The grain size ( $G_a$ )is determined using linear intercept method [12]:

$$G_a = \frac{3L}{2MN} \quad (3.4)$$

where ‘L’ is the line length, ‘N’ is the number of grains intercepting the test line;’ M’ is the magnification. ‘ $G_a$ ’ is found to be altering between 196to 235nm. This confirms the presence of microspheres.

**b.TEMAnalysis(Surface Morphology Property):**

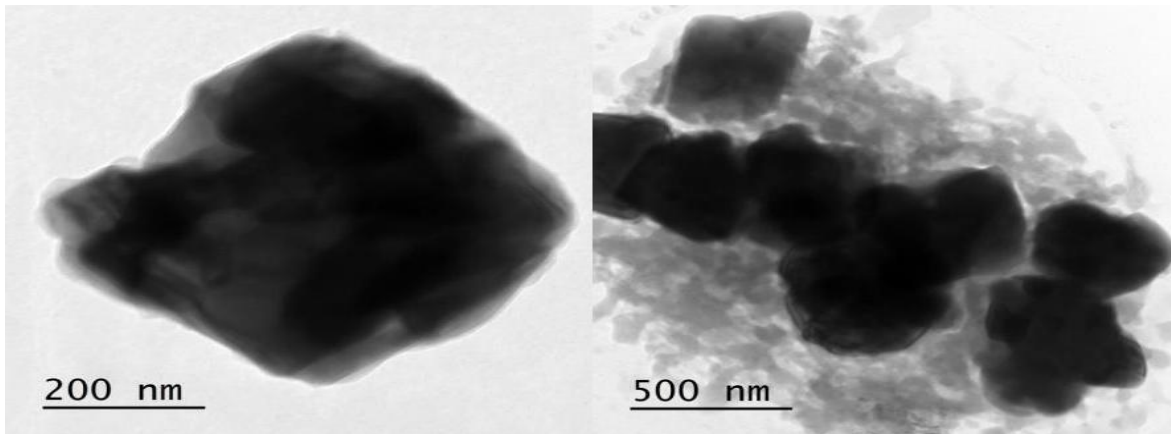


**Fig.5TheTEM photos of BTnanoparticles**

TEM generally provides the information about the existence of nano-particles. In this investigation the TEM images of BT nano-particles are shown in Fig.3.5. It is seen from Fig.5 that all BT nano particles are of spherical shape. The particle size is varying between 183 to 207 nm. In TEM images a weak-agglomeration is identified due to the less magnetisation behaviour among the BT nano particles.

### 3.a. FTIR Analysis (Optical Property)

The FTIR absorption spectra of synthesized BT nano-particles are recorded in the range of 4000 to 400  $\text{cm}^{-1}$  as depicted in Fig 6. Two kinds of metal oxide (M-O) stretching vibrations are detected in the range of 400 to 520  $\text{cm}^{-1}$ . This ensures the formation of perovskite BT structure. A narrow absorption band is noticed around 412  $\text{cm}^{-1}$  while broad absorption band, around 513  $\text{cm}^{-1}$ . These two absorption bands reflect the presence of Ba-O and Ti-O bonds. In addition few peaks are detected at 1122  $\text{cm}^{-1}$ , 1360  $\text{cm}^{-1}$  and 2853  $\text{cm}^{-1}$ . The peaks at 1124  $\text{cm}^{-1}$  and 1362  $\text{cm}^{-1}$  are associated to the bending vibrations of oxygen and hydrogen (O-H) that can be observed from the absorption of O-H by the BT nano-particles [13]. Another absorption peak is at 2852  $\text{cm}^{-1}$  is attributed to the intra-molecular stretching modes that occur from distinct properties of hydrogen bonding [13] within the frame network of perovskite structure.

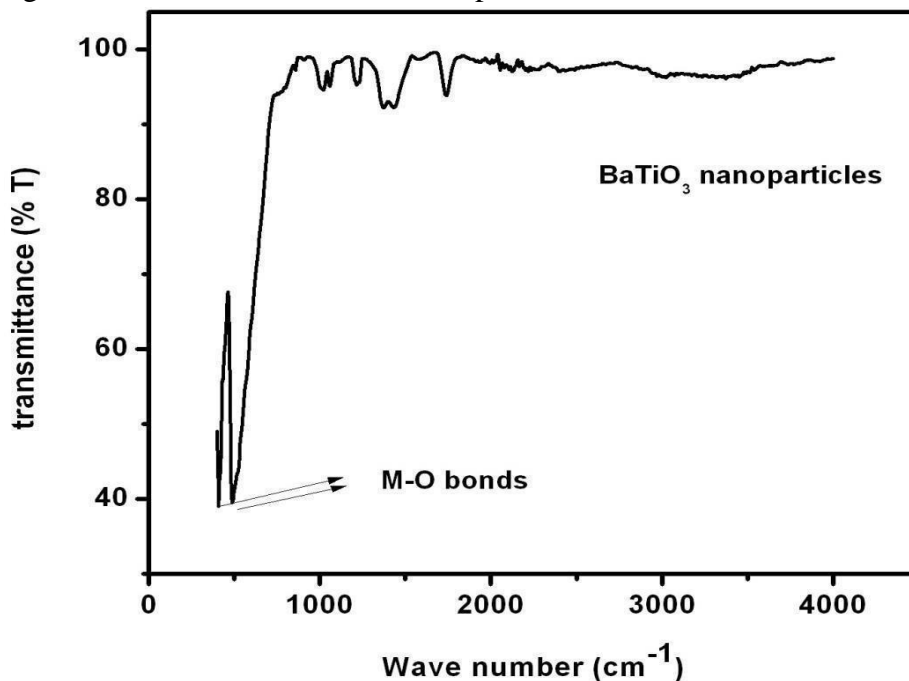


Fig.6 The FTIR spectra of BT nanoparticles

### 3.b. UV-Visible Spectral Analysis (Optical Property):

The difference reflectance spectrum (Fig.7) is recorded in the range of 500-2500 nm for evaluating optical and gap of powder samples. The Kubelka –Munk function of reflectance  $F(r)$  is used to determine band gap [12].

$$F(r) = \frac{(1-r)^2}{2r} \quad (3.5)$$

The absorption coefficient ( $\alpha$ ) is directly proportional to  $F(r)$  and hence an equation to find band gap can be written as follows [12]:

$$(\alpha h\nu)^n = m(h\nu - E_g) \quad (3.6)$$

where ‘m’ is energy-independent constant that depends on transition probability.  $E_g$  is optical band gap energy.  $n$  depends on the kind of transition i.e.,  $n=2$  for direct transition,  $2/3$  for direct forbidden transition,  $1/2$  for indirect transition and  $1/3$  for indirect forbidden transition, and  $h\nu$  is

photon energy. In this study  $n = 2$  is taken for the direct transition [12]. The  $E_g$  value is considered as extrapolated tangent value towards x-axis for  $(\alpha h\nu)^2$  versus photon energy  $h\nu$  (eV) plot as  $\alpha$  tends to zero. The maximum absorption wavelength ( $\lambda_m$ ) for BT nano-particles is shown in Fig 8. It is observed from figure that the  $\lambda_m$  value is acquired to be 340 nm for the BT nanoparticles. The optical band gap is found to be 3.23 eV and is consistent with previously reported data [8].

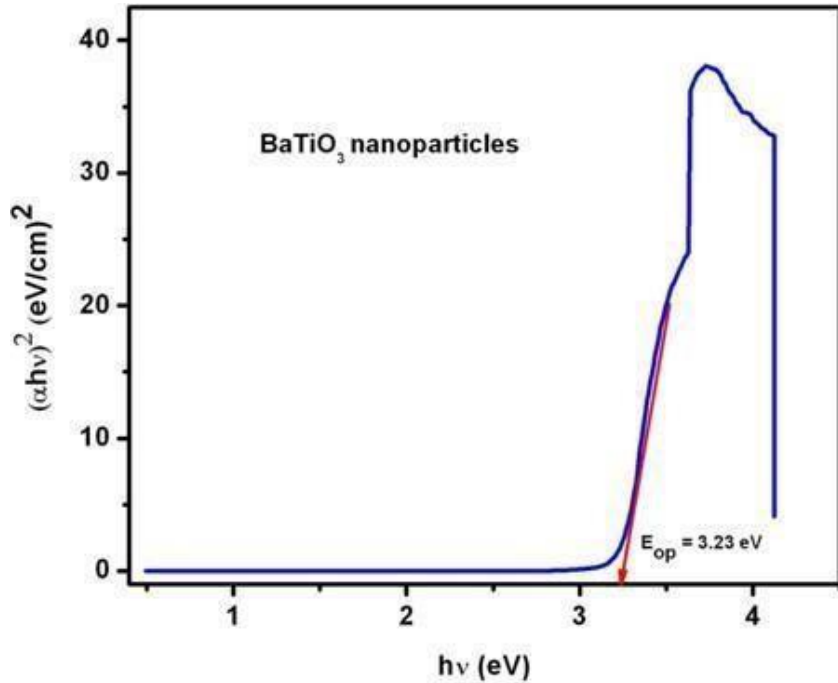


Fig.7 The  $\alpha h\nu$  versus photon energy of BT nanoparticles

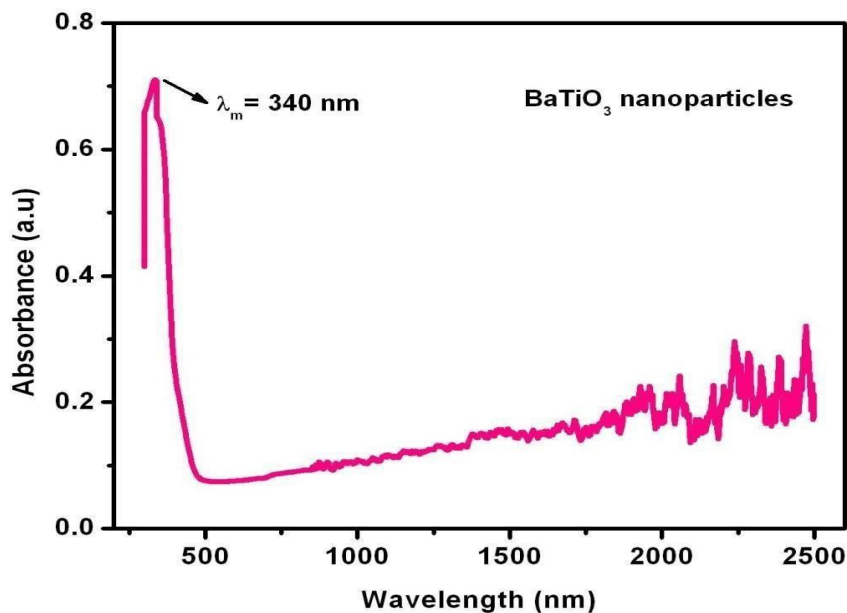


Fig.8 The absorption spectra of BT nanoparticles



**Conclusions:**

The BaTiO<sub>3</sub> nanoparticles were prepared by hydrothermal technique. The diffraction pattern revealed the perovskite BT cubic structure. The size of spherical grains is observed to be altering between 193 to 235 nm. The TEM study shows the agglomerated spherical nanoparticles. The presence of metal oxide bonds (M-O) were evaluated from Fourier transform infrared spectra. The UV-Visible spectrum attributes the optical band gap energy of 3.23 eV.

**Conflicts of Interest**

The author declares that there are no conflicts of interest regarding the publication of this review.

**Acknowledgements**

Author would like to thankful to Department of physics MALD gdc gadwal , palamure university, Nano science research lab and Institute of nano science and technology , for providing support and encouragement to carry out the study.

**References**

1. Gianni Ciofania, Leonardo Ricotti, Claudio Canalec, Delfo DAlessandro, Stefano Berrettini, Barbara Mazzolai, Virgilio Mattoli, Effects of barium titanate nanoparticles on proliferation and differentiation of rat mesenchymal stem cells, *Colloids and Surfaces B: Biointerfaces* 102 (2013) 312–320
2. Song Wei Lu, Burtrand I. Lee, Zhong Lin Wang, William D. Samuels, Hydrothermal synthesis and structural characterization of BaTiO<sub>3</sub> nanocrystals, *Journal of Crystal Growth* 219 (2000) 269-276 M.H. Frey, D.A. Payne, Grain-size effect on structure and phase transformations for barium titanate, *Physical Review B* 54 (1996) 3158.
3. J. Wang, J. Fang, S.C. Ng, L.M. Gan, C.H. Chew, X. Wang, Z. Shen, Ultrafine Barium Titanate Powders via Micro emulsion Processing Routes., *Journal American Ceramic Society* 82 (1999) 873-881.
4. W.S. Cho, Structural evolution and characterization of BaTiO<sub>3</sub> nanoparticles synthesized from polymeric precursor, *Journal of Physics and Chemistry of Solids* 59 (1998) 659-666.
5. Y. Ma, E. Vilen, S. Suib, P.K. Dutta, Synthesis of Tetragonal BaTiO<sub>3</sub> by Microwave Heating and Conventional Heating, *Chemistry Materials* 9 (1997) 3023-3031.
6. S. Selvarajan, Nagamalleswara Rao A, A Chandrasekhar, Sang-Jae Kim, Unconventional active biosensor made of piezoelectric BaTiO<sub>3</sub> nanoparticles for biomolecule detection, *Sensors and Actuators B: Chemical* <http://dx.doi.org/10.1016/j.snb.2017.07.159>
7. Monika Singh, B.C. Yadav, Ashok Ranjan, Manmeet Kaur, S.K. Gupta, Synthesis and characterization of perovskite barium titanate thin film and its application as LPG sensor, *Sensors and Actuators B: Chemical*, <http://dx.doi.org/10.1016/j.snb.2016.10.018>
8. M. Maddaiah, K. Chandra Babu Naidu, D. Jhansi Rani, T. Subbarao, Synthesis and Characterization of CuO-Doped SrTiO<sub>3</sub> Ceramics, *Journal of Ovonic Research* 11 (2015) 99-106.
9. K. Chandra Babu Naidu, W. Madhuri, Microwave processed NiMg ferrite: Studies on structural and magnetic properties, *Journal of Magnetism and Magnetic Materials* 420 (2016) 109–116 M. Maddaiah,

- K. Chandra Babu Naidu, D. Jhansi Rani, T.Subbarao, Synthesis and Characterization of CuO-Doped SrTiO<sub>3</sub> Ceramics, Journal of Ovonic Research 11 (2015) 99- 106.
10. K. Chandra Babu Naidu, W. Madhuri, Microwave processed NiMg ferrite: Studies on structural and magnetic properties, Journal of Magnetism and Magnetic Materials 420 (2016) 109–116
11. V. N. Reddy, K. C. Babu Naidu, T. Subbarao, structural, optical and ferroelectric properties of BaTiO<sub>3</sub> ceramics, Journal of Ovonic Research 12 (2016) 185-191
12. Chandra Babu Naidu K., Madhuri W., Microwave assisted solid state reaction method: Investigations on electrical and magnetic properties NiMgZn ferrites, Materials Chemistry and Physics 181 (2016) 432-443
13. K Chandra Babu Naidu and W. Madhuri, Hydrothermal synthesis of NiFe<sub>2</sub>O<sub>4</sub> Nanoparticles: structural, Morphological, optical, electrical and magnetic properties, bulletin of Material Science 40(2017) 417–425.